Polyoxometalate-based hybrid mesostructured catalysts for green epoxidation of olefins

Z. Karimi, A.R. Mahjoub [*], S.M. Harati

Department of Chemistry, Tarbiat Modares University, 14115-175 Tehran, Iran

ARTICLE INFO

ABSTRACT

Novel hybrid polyoxometalates (POM) of α-$H_3PW_{12}O_{40}$·nHMPA and α-$H_3PMo_{12}O_{40}$·nHMPA composed of α-$H_3PW_{12}O_{40}$ and $H_3PMo_{12}O_{40}$ heteropoly acides (HPAs) and hexamethylphosphoramide (HMPA) organic substrate has been synthesized and purified. SBA-15 mesoporous silica is synthesized, using P123 surfactant via hydrothermal method, and functionalized with aminopropyl functional groups via grafting method. The synthesized mesostructured supports are used for intercalation of the hybrid POMs. The parent Keggin HPAs are also immobilized within the supports to perform closer and more efficient investigation. After characterization, effect of functional groups on immobilization pattern and quality is taken into consideration. The mesostructured organic–inorganic hybrid materials are characterized using X-ray diffraction (XRD), scanning electron microscopy (SEM), transmission electron microscopy (TEM), atomic absorption, and FT-IR analysis. The newly designed hybrid catalysts are investigated for heterogeneous epoxidation of olefins. Effects of temperature, oxidant, and catalyst amount are studied and the reaction conditions are optimized. An interpretation of the differences in the catalytic activity of the precursors is put forward and their catalytic activity is compared with their HPA counterparts. Furthermore, effects of functionalization on catalyst activity, stability, and reusability are taken into consideration. Results reveal that the designed mesostructured POM based hybrid catalysts can selectively and efficiently epoxidize olefins in presence of hydrogen peroxide as oxidant. The catalysts are shown to be heterogeneous and reusable without significant loss of activity in the proceeding rounds.

© 2011 Elsevier B.V. All rights reserved.

1. Introduction

Production of epoxides is of growing interest in chemical and petrochemical industries due to their applications as organic intermediates in pharmaceutical synthesis and as monomers in production of various functional polymers [1–5]. However, epoxidation reaction sometimes requires hazardous chemicals which leave acid wastes. Therefore, designation of efficient heterogeneous catalysts is an important step to going green, which involves both rigorous control of the surface chemistry and geometry at micro, meso, and macroscales. Besides, high active phase dispersion is inevitable for fast mass transfer of reactants to the active catalytic sites. Thus, much interest has been driven to production of unique mesostructured systems with uniform and tailored pore structure.

Polyoxometalates (POMs) are an immense class of oxygen bridged metal cluster anions of mainly tungsten and molybdenum [6,7]. Some POMs, such as phosphotungstic acid ($H_3PW_{12}O_{40}$, PW) and phosphomolybdic acid ($H_3PMo_{12}O_{40}$, PMo), have a soccer ball-shaped Keggin structure [8] with a molecular size of ca. 1 nm [9] in which a central PO_4 tetrahedron is surrounded by a $W_{12}O_{36}$ or $Mo_{12}O_{36}$ shell [6,10]. They have attracted much attention as environmentally benign acids and efficient and highly selective electrophilic and oxidation catalysts [10,11]. Besides, versatility and accessibility of Keggin series have led to synthesis of various hybrid materials based on the Keggin structure [12,13]. In the last few years there have been a rapidly growing number of reports in the literature addressing the use of polyoxometalate as both homogeneous and heterogeneous catalysts [6,14–16]. However, to the best of our knowledge, only few reports are involved with catalytic applications of organic–inorganic hybrid Keggin POMs [13].

Since the polyoxometalates were found highly efficient for epoxidation of olefins by Venturello et al. [17,18] and Ishii et al. [19,20] in 1980s, various H_2O_2-based epoxidation systems have been efficiently catalyzed by POM based systems [21,23]. However, there exist some drawbacks about POMs catalysts: their thermal stability is relatively low and they are extremely soluble in polar solvents, which thus results in separation problems. Moreover, surface area of unsupported POMs is usually low (1–$10 \text{ m}^2/\text{g}^{-1}$) which is an important restriction for catalytic systems. All these limitations may be satisfied by grafting POMs within proper

* Corresponding author. Tel.: +98 21 82883443; fax: +98 21 88009730.
E-mail address: mahjouba@modares.ac.ir (A.R. Mahjoub).

heterogenizing supports, which is a great step to designation of efficient heterogeneous POM based catalysts [22–25].

A new paradigm in heterogeneous catalysis is made possible by application of MCM-type [25,26] and SBA-type [27] mesoporous materials as appropriate host matrices for finely dispersion of POM species within the uniform and tailored pores and channels [28,29] and efficient improvement of their catalytic activity [19,20].

SBA-15 mesoporous silica (prepared using neutral block copolymer), with well ordered hexagonal arrays of cylindrical channels, narrow pore size distributions, remarkable thermal stability (up to 1000 K), large uniform pore size (5–30 nm), high surface area (600–1000 m^2/g), thick silica walls (3.1–6.4 nm) [23,30], and a large number of silanol groups at the surface of its channels [31], serves as an intriguing support for the purpose. Furthermore, SBA-15 mesopores are interconnected by micropores [32,33], enabling the pore surfaces to be accessed in three dimensions in catalytic reactions.

This efficient support may be modified with 3-aminopropyl-triethoxysilane (APTES) via grafting method, in which hydroxyl groups of SBA-15 react with the organosilane to form a NH_2 functional group [34–37]. This process is an important extension, since it allows significant modification of physical and chemical properties. Furthermore, rational design and tailoring of hydrophobicity, adsorption characteristics and reactivity is possible with the hybrid organic/inorganic material. In addition to these merits, functional groups enhance the interactions of POM with the support material either by physical forces (i.e. hydrogen bonding and electrostatic interactions) or chemical bonding and allow higher and more stable loading [29,38,39].

In this work, we report synthesis of novel organic–inorganic hybrid materials with hexamethylphosphoramide (HMPA), as the organic group, and tungsten and molybdenum Keggin POMs, as the inorganic foundation. The polyoxometalate has the capacity to be reduced and can form crystals, and HMPA, with a large dipole moment, has unusually high basicity [40,41] and can form complex with polyoxometalate acids. The newly synthesized complexes are then incorporated within pristine and functionalized SBA-15 mesostructured supports and studied as heterogenous catalytic systems for oxidation of olefins. Oxidation conditions are optimized and heterogeneous nature, efficiency, selectivity, and reusability of the catalysts are truly assessed.

2. Experimental

2.1. Chemicals

All materials are of commercial reagent grade and are purchased from Merck Company. P123 (poly(ethylene oxide)–poly(propylene oxide)–poly(ethylene oxide) (EO20–PO70–EO20)) is purchased from Aldrich Company. Tungstophosphoric Acid α-H_3[$PW_{12}O_{40}$] (labeled as HW) is produced via the procedure reported earlier [42]. Molybdophosphoric Acid α-H_3[$PMo_{12}O_{40}$] (labeled as HMo) is synthesized according to literature [43].

2.2. Catalyst preparation

2.2.1. Synthesis of HMPAW ($H_3PW_{12}O_{40}·n[C_6H_{18}N_3OP]$)

Phosphotungstic acid (2 g equal to 0.694 mmol) is dissolved in 1:1 mixture of ethanol and water and HMPA (0.385 g equal to 2.08 mmol) is then added to the solution. The resulting yellow transparent solution is left to produce yellow crystals of $H_3PW_{12}O_{40}·n[C_6H_{18}N_3OP]$ labeled as HMPAW.

2.2.2. Synthesis of HMPAMo ($H_3PMo_{12}O_{40}·n[C_6H_{18}N_3OP]$)

Phosphomolybdic acid (1.65 g equal to 0.902 mmol) is dissolved in a 1:1 mixture of water and ethanol and HMPA solution in ethanol (1 g equal to 5.41 mmol) of is then added to the solution and stirred for an hour. The resulting yellow precipitate is collected and sucked as dry as possible on a fritted-glass funnel. The precipitate is recrystalized from an acetonitrile solution to yield orange crystals of $H_3PMo_{12}O_{40}·n[C_6H_{18}N_3OP]$ labeled as HMPAMo.

2.2.3. Synthesis of SBA-15

Synthesis of SBA-15 is conducted according to the literature [32]. Pluronic P123 is used as a template, and the silica source is TEOS, which is added drop wise to an acidic P123 aqueous solution and then stirred at 40 °C for 24 h at 600 rpm. The reaction mixture is acidified by adding HCl aqueous solution. The molar ratio of the reaction mixture is 1TEOS:0.0168 P123:5.8HCl:155H_2O. The powder is recovered by filtration, dried overnight, and further calcined at 600 °C for 6 h.

2.2.4. Synthesis of SBA-15/NH_2

To prepare functionalized mesoporous supports via post-synthesis method, 1.0 g of pure calcined SBA-15 is reacted with 50 mL of 0.01 M solution of APTES in dried toluene under reflux for 8 h. The resultant white solid is filtered off, washed with dried toluene, dried under vacuum, and labeled as SBA/NH_2.

2.2.5. Immobilization of PMo on mesoporous supports

Preparation of novel materials based on silica and polyoxometalates is performed by the suspension of 1 g of mesoporous silica (SBA-15 or SBA/NH_2) in 10 ml of POM solution (0.7 M) in 1:1 mixture of acetonitrile and ethanol. The resulting mixture is gently stirred in 70 °C until equilibrium is reached (typically 24 h). The solid product is then centrifuged and washed several times with ethanol. The precipitate is then dried at room temperature and labeled as SBA/HW, SBA/HMo, SBA/HMPAW, SBA/HMPAMo, [SBA/NH_2]/HMPAW, [SBA/NH_2]/HMPAMo.

2.3. Characterization of the samples

Characterization of the synthesized organic–inorganic hybrid mesoporous materials is performed by different conventional techniques. X-ray powder diffraction (XRD) data are acquired on a Philips X-Pert diffractometer using Cu Kα radiation. TEM images are acquired using Loe 906 Microscope operating at 100 kV. Atomic Absorption data are acquired by contrAA 700 using flam technique. FT-IR spectra are recorded on a Nicolet, IR 100 FT-IR Spectrometer.

2.4. Catalytic experiments

Catalytic epoxidation reactions are performed in a round bottom flask in an oil bath under magnetic stirring (400 rpm). Unless otherwise specified, all oxidation reactions are carried out under reflux at atmospheric pressure with 1 mmol of olefin, 2 ml of 30% H_2O_2 as oxidant, 1 ml of dichloromethane as solvent, n-dodecane (0.1 mmol) as internal standard for product quantification, and 0.025 g of hybrid mesostructured catalysts. Catalytic reactions are monitored using Gas chromatography, GC, HP5890 chromatogram.

3. Results and discussion

3.1. Immobilization of POMs within SBA-15 and SBA-15-NH_2

The immobilization pattern profits from an acid–base interaction between the POMs (as Brønsted acid) and silanol groups present at the surface and inside the channels of the mesoporous silica (as the base) [35,36]. In fact, chemically active surface silanol groups (–Si–OH) of silica matrix are protonated in an acidic medium (produced by POMs) to form –Si–OH_2^+ groups [44], which

serves as a counter ion for the $(-SiOH_2^+)(H_nP_pM_mO_q^- \cdot HMPA)$ polyanion [45–47] (Scheme 1). Furthermore, hydrogen bondings are present between $M=O_t$, $M–O_c$, $M–O_e$, $P=O$ and amine groups of HMPA with HO–Si. These interactions ensure a stable and non-physically adsorption pattern for POM intercalation within the pristine SBA silica support.

As for SBA-15-NH$_2$/POMs, the functional group promotes chemical immobilization of POM by taking advantage of its overall negative charge, producing $(-SiNH_3^+)(H_nP_pM_mO_q^- \cdot HMPA)$ polyanion (Scheme 1). Besides, stronger hydrogen interactions are produced with aminopropyl functionalized support, compared to the non-functionalized one. Hence, a more stable heterogeneous catalyst is produced with higher amount of guest molecules retained within the support.

3.2. Characterization of the hybrid materials

Low angle powder X-ray diffraction (XRD) patterns of pure, functionalized, and POM containing SBA-15 (Fig. 1A) confirm the structural maintenance upon both functionalization and incorporation of guest molecule. The three distinct Bragg diffractions (1 0 0), (1 1 0), and (2 0 0), are characteristics of a highly ordered two-dimensional hexagonal mesoscopic structure of pure SBA-15 [48]. Presence of the reflections in all diffractograms is indicative of the hexagonal pore structure retainment after incorporation of the guest molecules. The intensity and resolution of reflections is based solely on the degree of ordering in the material's pore array and arises from the electron density gradient between the walls and pores. POM immobilization within the mesoporous host reduces the order of the mesostructured system and leads to increased phase cancellation between X-rays scattered from the walls and pores regions. Thus, a decrease in the intensity of the Bragg reflections in the low angle region is evidenced [49]. Similar pattern is observed for the functionalized hybrid materials (Fig. 1B). No peaks characteristic of POM is detected in the wide angle region. This may be attributed to the fine dispersion of the POM species within the copious pores

and channels of the mosoporous supports. Actually, separate detectable crystal phases of material are differentiated based on XRD patterns. When the impregnated guest species are finely dispersed within the support, they does not give rise to a separate crystal phase and hence, no peaks corresponding to the bulk phase of the guest molecules is detected in XRD [50]. The d_{100}-spacing (calculated from Bragg equation) and unit cell parameters (calculated using $a_0 = 2d_{100}/\sqrt{3}$) of the designed materials are determined based on the low-angle XRD patterns (Table 1).

According to scanning electron microscopy (SEM) images (Fig. 2a–c), morphology of SBA supports have remained intact both after functionalization and POM immobilization. Transmission electron microscopy (TEM) is also applied to observe the extent of order in these materials and also the shape and regularity of channels. The micrographs demonstrate that the hexagonal ordered channel structure of parent SBA-15 has been retained in the designated hybrid materials (Fig. 2d and e).

The amount of incorporated POMs is estimated based on atomic absorption data (Table 1). As expected, aminopropyl functional group improves immobilization process and higher content of POM is immobilized within the functionalized support.

FT-IR analysis is applied to shed light on the structure of HMPAW and HMPAMo species (electronic supplement and Fig. 3A(c and e)). Comparing the IR spectra of the parent heteropoly acid with the corresponding HMPA hybrid material, the vibrational band corresponding to the P=O bond of HMPA exhibits a red-shift from 1203 cm^{-1} in HMPA to 1172 cm^{-1} in the hybrid POMs (Table 2). This suggests that the every HMPA has produced hydrogen bonding with protons of the parent heteropoly acid [13]. This combination weakens the P=O band and strengthens the P–N band of the organic group.

FT-IR spectra of pristine, functionalized, and POM impregnated SBA mesoporous supports are studied for structural characterization purposes (Fig. 3A). Pristine SBA-15 gives a broad low-frequency band at 3427 cm^{-1} due to those silanol groups or silanol nests with cross hydrogen bonding interactions. Bands
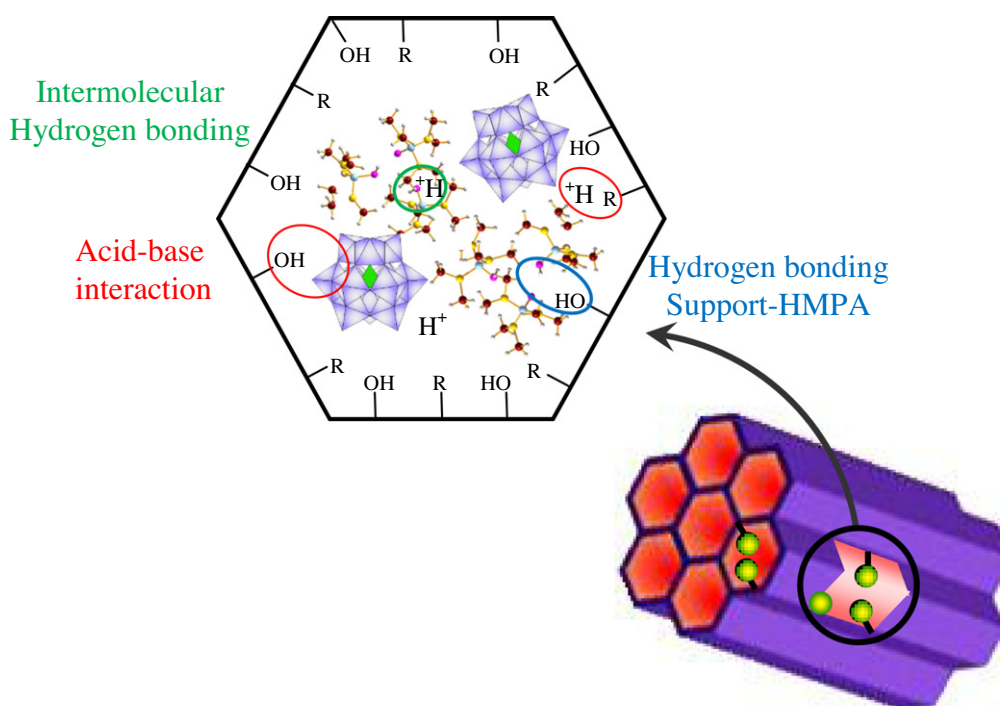
Scheme 1. POM immobilization drill within SBA-type mesostructured supports. Some types of interactions are shown. For nonfunctionalized supports R = –OH and for functionalized ones R = ⌒⌒NH$_2$.
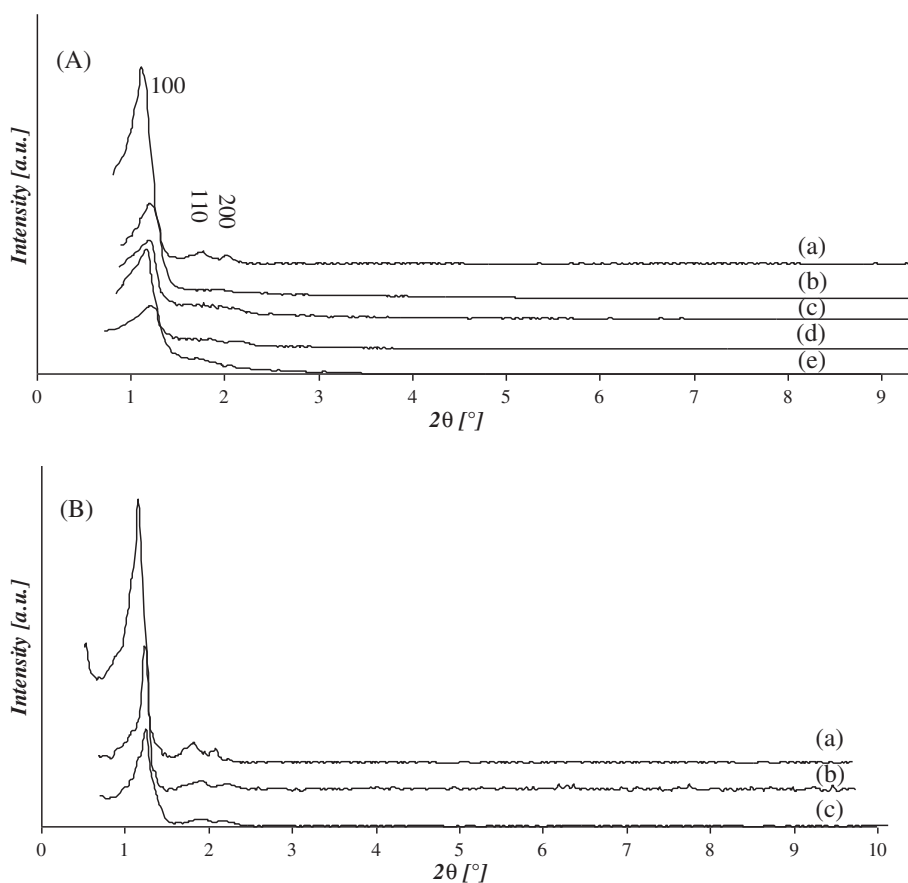
Fig. 1. Low-angle XRD patterns of: (A) (a) SBA-15, (b) SBA/HMPAW, (c) SBA/ HMPAMo, (d) SBA/HW, (e) SBA/HMo; (B) (a) SBA/NH₂, (b) [SBA/NH₂]/HMPAW; (c) [SBA/NH₂]/HMPAMo.

Table 1
Structural properties and chemical composition of mesostructured hybrid materials.

Sample	d_{100} (nm)	Unit cell parameter (nm)	W or Mo content (wt.%)
SBA-15	7.95	9.2	–
SBA-15/NH₂	7.3	8.4	–
SBA/HW	7.6	8.8	17.2
SBA/HMo	7.5	8.7	12.2
SBA/HMPAW	7.3	8.4	16
SBA/HMPAMo	7.4	8.6	8.69
[SBA/NH2]/HMPAW	7.2	8.3	21.9
[SBA/NH2]/HMPAMo	7.1	8.2	13.8

corresponding to Si–O–Si are detected at 1079 cm⁻¹ and 809 cm⁻¹. As for the aminopropyl functionalized support, bands corresponding to NH₂ functional group are found around 2925, 1510 and 691 cm⁻¹ (Fig. 3B). The primary structure of unsupported POMs is also identified by distinct IR bands which are summarized in Table 2. Actually, clear observation of POM is hindered as a result of the strong background of silica support. Owing to the overlap of 868 cm⁻¹ M–O–M and P–O bands with those of Si–O–Si stretching vibrations of mesoporous supports, only few bands corresponding to POM are discernable after immobilization within the supports. Besides, the slight shift in the position of peaks serves as an evidence for interaction between the mesostructured host and guest molecules.

3.3. Epoxidation reaction

3.3.1. Optimizing the reaction conditions

Reaction conditions are optimized in presence of SBA/HMPAW as a model for other synthesized POM containing heterogeneous catalysts and effects of solvent, catalyst amount, temperature, and oxidant are taken into consideration.

Dichloromethane, acetonitrile, and methanol are studied as models to study the solvent effect on the epoxide yield (Table 3). All the reactions are carried out under identical conditions with 0.025 g catalyst, 1 mmol substrate (cyclooctene), 2 ml hydrogen peroxide, and 1 ml solvent. It seems that dichloromethane is the best solvent for the purpose.

In order to optimize the catalyst amount, catalytic reactions are performed using different amounts (0.01, 0.025, 0.05 g) of SBA/ HMPAW catalyst. Other parameters are kept constant (1 mmol cyclooctene, 2 ml hydrogen peroxide, and 1 ml CH₂Cl₂) and the systems are refluxed for 12 h. Higher epoxides yield is achieved by enhancing the catalyst amount from 0.01 g to 0.025 g (Table 3). Further increase in the catalyst amount produces no significant influence. Thus, the following experiments are carried out with 0.025 g of catalyst.

Temperature can also be important for achieving the optimum result. To study the effect, reaction is performed at room
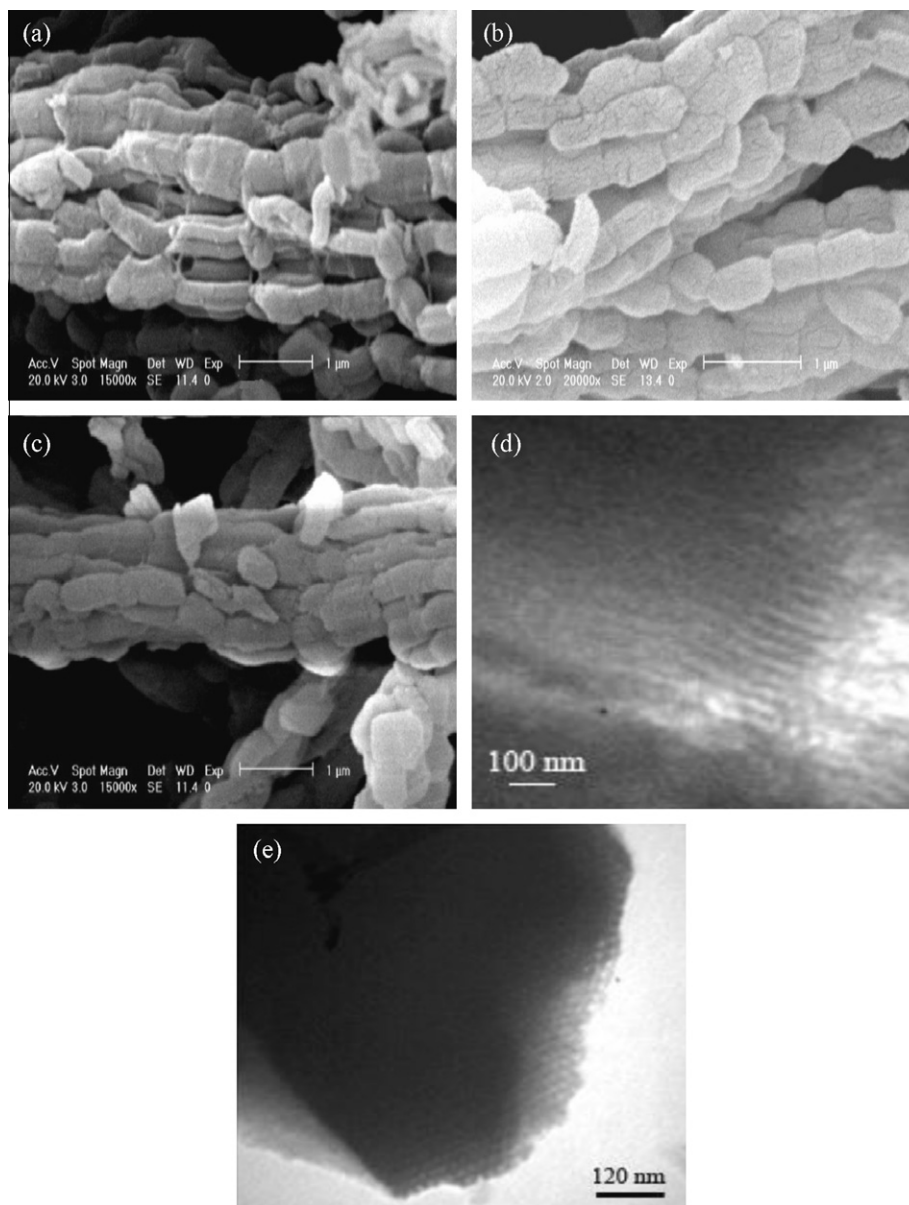
Fig. 2. SEM images of: (a) SBA/HMPAW, (b) [SBA/NH$_2$]/HMo, and (c) SBA/HW, and TEM images of (d) SBA/HMPAMo and (e) [SBA/NH$_2$]/HMPAW.

temperature and under reflux conditions with 0.025 g of SBA/HMPAW catalyst, 1 mmol of cyclooctene, 2 ml hydrogen peroxide, and 1 ml CH$_2$Cl$_2$. The oxidation reaction proceeds much slower at room temperature and reflux temperature is shown to be more proper for the purpose (Table 3).

Either tertiary butyl hydrogen peroxide (TBHP) or H$_2$O$_2$ can be applied as oxidant for epoxidation of olefins. Better conversion rates are evidenced in presence of H$_2$O$_2$ (Table 3). Besides, hydrogen peroxide is much preferred as an eco-friendly green oxidant which generates only water as a by-product and has a high content of active oxygen species [52–55]. Hydrogen peroxide is also more desirable because of safety and ease of handling. It's noteworthy that in absence of oxidant, no peroxo is produced and the oxidation does not occur.

3.3.2. Effect of the nature of catalyst

Catalytic activity of the newly designed hybrid mesostructured materials is studied for epoxidation of olefins. Results are summarized in Table 4. All the catalytic systems are shown to be highly active and selective towards epoxide product. Blank reaction is carried out to specify the role of catalyst. No conversion is achieved in the absence of catalyst. Similar oxidation reactions are also carried out with bare silica supports and only negligible catalytic activity is evidenced (about 4% conversion for cyclooctene). These clearly imply that the immobilized POM species are responsible for the high oxidation activity of the hybrid catalysts. Besides, the large pores and channels of the SBA support permit diffusion of relatively large cyclic alkenes and epoxidation proceeds selectively inside copious pores and channels of the mesostructured support.

Generally, the reaction is believed to proceed via the mechanism postulated for Keggin type POMs. Monomeric, dimeric, and tetrameric peroxo species are generated by the reaction of polyoxometalates with hydrogen peroxide, and the peroxo species are postulated to be the catalytically active species for epoxidation of olefins with POM/H$_2$O$_2$ system [51,56,57]. Closer monitoring of the oxidation process indicates that the nature of addenda atoms plays a vital role in activity of the hybrid catalysts. Tungsten-based systems exhibit higher reactivity compared to molybdenum
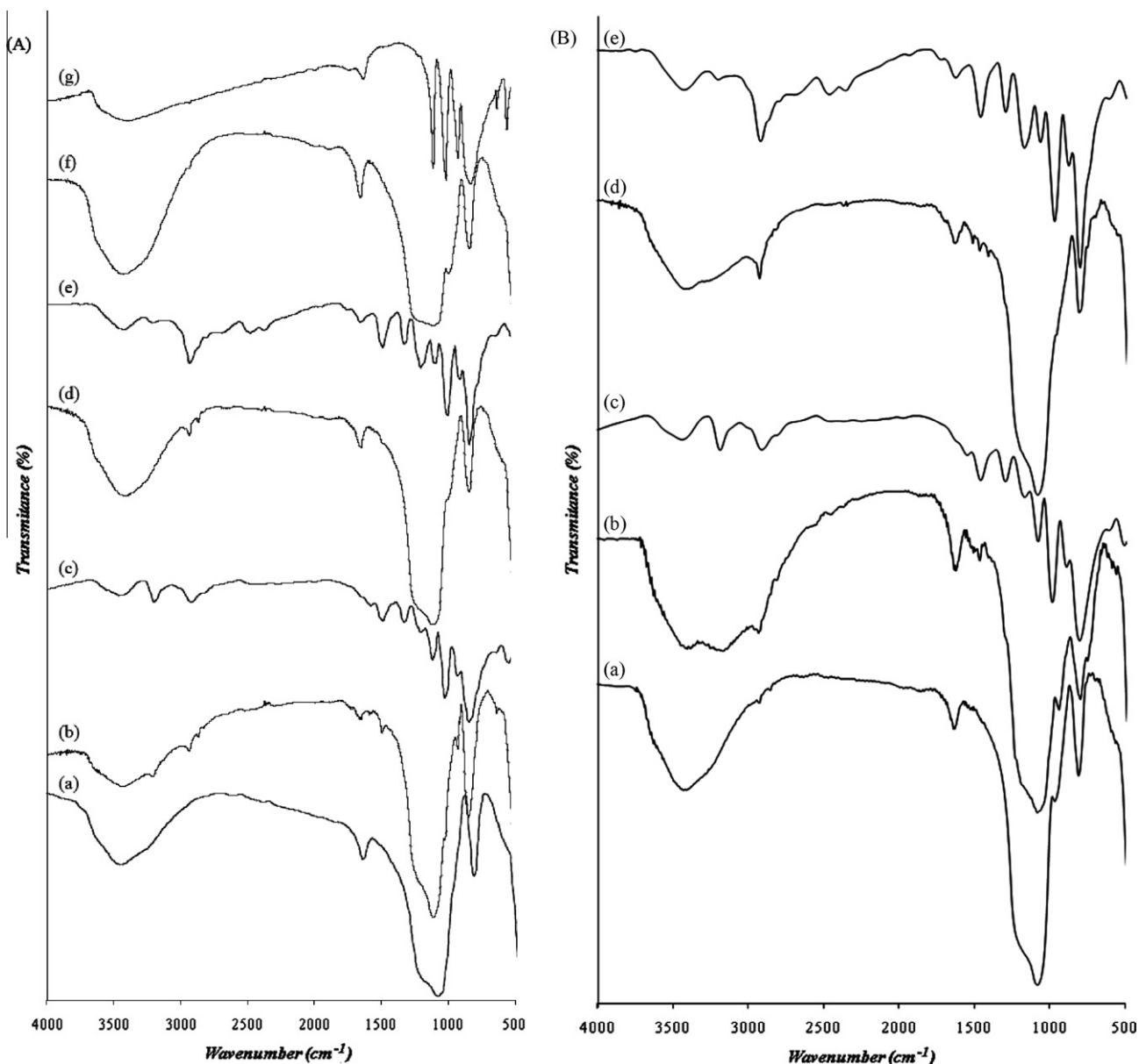
Fig. 3. FT-IR spectra of: (A) (a) SBA-15, (b) SBA/HMPAW, (c) HMPAW, (d) SBA/HMPAMo, (e) HMPAMo, (f) SBA/HW, (g) HW, and (B) (a) SBA/NH2, (b) [SBA/NH₂]/HMPAW, (c) HMPAW, (d) [SBA/NH₂]/HMPAMo and (e) HMPAMo.

Table 2
Position of FT-IR characteristic bonds corresponding to unsupported POMs and HMPA.

Compound	FT-IR characteristic bands
HMPA	980 cm^{-1} (P–N), 1203 cm^{-1} (P=O), 1290 cm^{-1} (C–N)
HW	795 cm^{-1} (W–O$_c$–W), 890 cm^{-1} (W–O$_b$–W), 982 cm^{-1} (W=O$_d$), 1080 cm^{-1} (P–O$_a$)
HMo	789 cm^{-1} (Mo–O$_c$–Mo), 868 (Mo–O$_b$–Mo), 964 cm^{-1} (Mo=O$_d$), 1064 cm^{-1} (P–O$_a$) [48]
HMPAW	609 cm^{-1} (bending P–O), 807 cm^{-1} (W–O$_c$–W), 895 cm^{-1} (W–O$_b$–W), 987 cm^{-1} (W=O), 1081 cm^{-1} (P–O$_a$), 1172 cm^{-1} (P=O), 1298 cm^{-1} (C–N), 1462, 2913 & 3189 cm^{-1} (–CH₃)
HMPAMo	609 cm^{-1} (bending P–O), 804 cm^{-1} (Mo–O$_c$–Mo), 878 cm^{-1} (Mo–O$_b$–Mo), 972 cm^{-1} (Mo=O), 1066 cm^{-1} (P–O$_a$), 1172 cm^{-1} (P=O), 1298 cm^{-1} (C–N), 1462, 2920 & 3209 cm^{-1} (–CH₃)

analogs. Actually, tungsten POMs are usually regarded as stronger acids compared to their molybdenum counterpart [58]. It seems that the epoxidation reaction rate and epoxides yield is controlled and determined by catalyst's acid strength [59]. Hence, tungsten POMs show higher catalytic activity. Speaking of the acid strength to justify our achievements, we decided to compare the catalytic performance of phosphomolybdic [55] and phosphotungstic acids

immobilized within SBA-15 for oxidation of cyclooctene as a model for other olefins (Table 4). As expected, SBA/W and SBA/Mo produce higher yield of epoxide, with SBA/W being more active. The higher activity of the SBA/W catalyst is clearly justified regarding its higher acidity. As mentioned before, in the hybrid POMs, the acidic protons of the parent heteropoly acids are engaged in a hydrogen bonding with the oxygen of the P=O group of HMPA.

Table 3
Optimization of the cyclooctene oxidation reaction conditions using SBA/HMPAW hybrid catalyst (1 mmol substrate, 0.1 mmol n-dodecane, 2 ml oxidant, and 1 ml solvent). Results are reported after 12 h of reaction.

Amount of SBA/HMPAW catalyst (g)	Solvent	Oxidant	Temperature	Conversion (%)
0.025	CH_2Cl_2	H_2O_2	reflux	71.5
0.025	CH_3CN	H_2O_2	reflux	64.3
0.025	MeOH	H_2O_2	reflux	58.4
0.01	CH_2Cl_2	H_2O_2	reflux	65.6
0.05	CH_2Cl_2	H_2O_2	reflux	71.8
0.025	CH_2Cl_2	H_2O_2	room temperature	54.7
0.025	CH_2Cl_2	TBHP	reflux	63.5

Hence, their acidity is reduced and as the reaction procedure is affected by this factor, lower catalytic activity is evidenced with the hybrid POM based systems.

Catalytic performance of the heterogeneous catalysts is also related to fine dispersion of the active catalytic species within the supports. Here, the immobilizing support and the nature of functional groups are shown to have crucial effect on oxidation process. Actually, as mentioned previously, functionalization improves sorption properties and guest incorporation within SBA-15 mesoporous host. Indeed, higher amount of Guest molecules are believed to be more finely dispersed via chemical immobilization within the NH_2 functionalized SBA-15, compared to the non-functionalized mesoporous. Thus, more catalytic active sites are available and oxidation reaction is more efficient. This is in accordance with the epoxidation results, higher epoxides yield is achieved with the aminopropyl functionalized systems (Table 4).

To study the oxidation procedure more closely, the reaction is performed under the optimized conditions (i.e. 0.025 g catalyst, 1 mmol cyclooctene, 2 ml H_2O_2, 1 ml CH_2Cl_2, 0.1 mmol n-dodecane under reflux) and epoxides yield is considered at different time intervals (Fig. 4). Interestingly, the reaction proceeds more slowly in presence of aminofunctionalized hybrid catalysts. This may be attributed to the hindrance and restrictions for diffusion of the reagent inside the pores and channels of the mesostructured catalyst. However, as mentioned above, higher yield is accomplished with the functionalized catalysts.

3.3.3. Recyclability of catalysts

To assess stability and reusability, catalysts are separated from the reaction mixture after each experiment, washed several times and dried before being applied in the subsequent run. During the second cycle of reaction with SBA/HMPAW and SBA/HMPAMo

Table 4
Catalytic performance of the designed mesoporous catalysts for epoxidation of olefins (0.025 g catalyst, 1 mmol substrate, 0.1 mmol n-dodecane, 2 ml H_2O_2, and 1 ml CH_2Cl_2). The data are reported after 12 h of reaction. * = TON (turnover number) is defined as mmol of epoxide/mmol POM.

| Catalyst	Substrate	Product	Conversion (%)	Selectivity to epoxide (%)	TON*
SBA/HMPAW	Cylopentene	Cylopentene oxide	76	97	409
	Cyclohexene	Cyclohexene oxide	77	89	376
	Cyclooctene	Cyclooctene oxide	71	99	394
	Cyclododecene	Cyclododecene oxide	79	99	435
SBA/W	Cyclooctene	Cyclooctene oxide	90	99	462
SBA/HMPAMo	Cylopentene	Cylopentene oxide	56	97	287
	Cyclohexene	Cyclohexene oxide	57	87	264
	Cyclooctene	Cyclooctene oxide	59	98	306
	Cyclododecene	Cyclododecene oxide	74	99	394
SBA/HMo	Cyclooctene	Cyclooctene oxide	88	99	332
[SBA/NH_2]/HMPAW	Cyclooctene	Cyclooctene oxide	79	99	321
	Cyclododecene	Cyclododecene oxide	88	98	347
[SBA/NH_2]/HMPAMo	Cyclooctene	Cyclooctene oxide	68	99	228
	Cyclododecene	Cyclododecene oxide	83	99	278
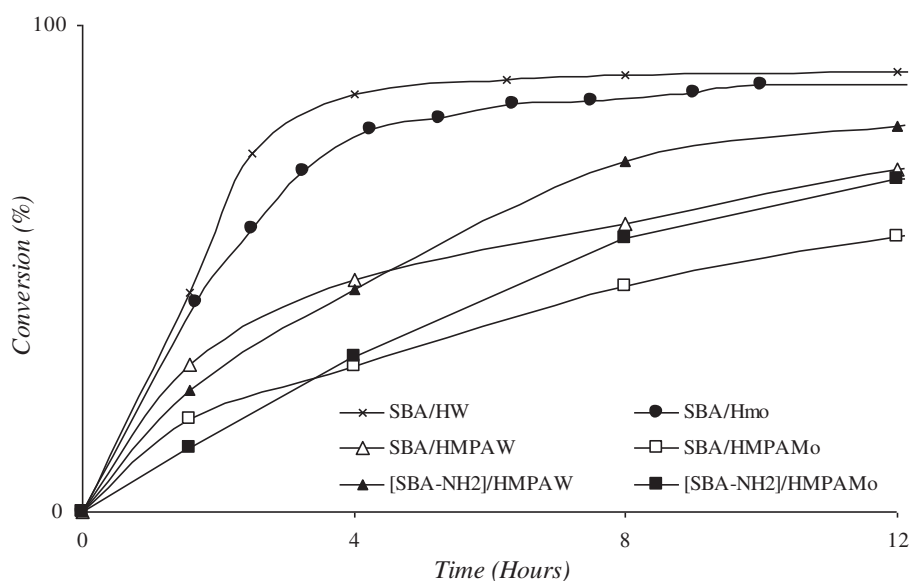
Fig. 4. Comparison of catalytic activity of heterogeneous mesostructured catalysts for epoxidation of cyclooctene (0.025 g catalyst + 1 mmol cyclooctene + 2 ml H_2O_2 + 1 ml CH_2Cl_2 + 0.1 mmol n-dodecane under reflux.).
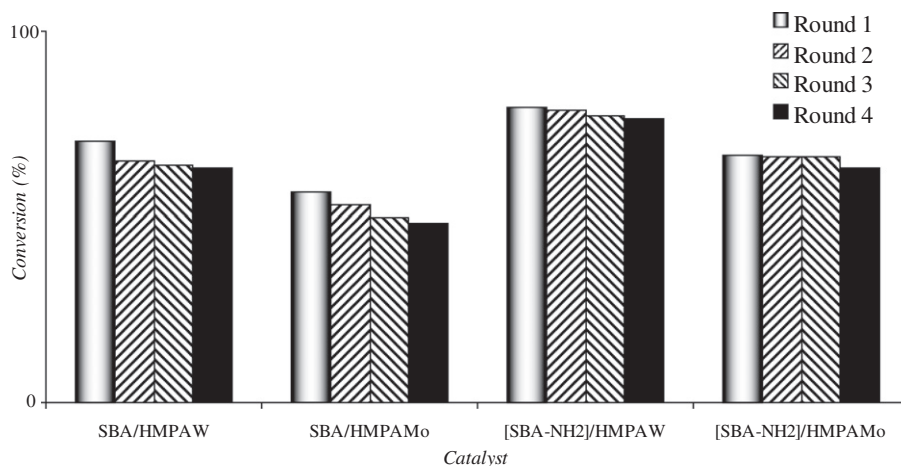
Fig. 5. Catalytic activity of heterogeneous catalysts during the recycling process for cyclooctene epoxidation.

catalysts, a slight reduction is evidenced in the epoxide yield (Fig. 5) which may be attributed to leaching of unstable immobilized POM. Nevertheless, the catalytic activity is nearly retained during the later runs. However, this activity loss is not evidenced with the functionalized hybrid catalysts. This is due to stronger chemical interactions between the hybrid POM and the support and hence, more efficient retainment of the catalytic active sites within the pore and channels of the functionalized support.

4. Conclusion

This work provides an efficient and easy method for designation of a novel and selective POM-HMPA hybrid heterogeneous catalysts for epoxidation of relatively large olefins. α-$H_3PW_{12}O_{40}\cdot n$HMPA and α-$H_3PMo_{12}O_{40}\cdot n$HMPA organic–inorganic hybrid POMs are synthesized. SBA-15 and SBA-15-NH_2 mesoporous silicas are also synthesized and characterized. The mesostructured porous materials are shown to be effective supports for immobilization of the hybrid POMs and their HPA analogs. XRD, SEM, and TEM analyses reveal that structure of mesoporous supports remains intact after POM grafting. Atomic absorption and FT-IR analyses confirm POM immobilization. Results reveal that the sorption property of the mesoporous support is improved by functionalization with NH_2 group.

The newly designed mesoporous hybrids are shown to combine catalytic activity of POMs with high surface area of mesoporous supports. Such kind of materials can be efficiently used as environmentally benign, green, and selective heterogeneous catalysts for epoxidation of olefins. The epoxidation reaction conditions are optimized and effect of chemical composition and structure is considered for both POM's and the immobilizing mesoporous support. Best catalytic results are achieved with 0.025 g of [SBA/NH_2]/HMPAW in presence of H_2O_2 oxidant CH_2Cl_2 solvent under reflux conditions. The hybrid catalysts are shown to be heterogeneous and reusable and may be recovered at least for four runs without any significant loss in activity.

Acknowledgment

Appendix A. Supplementary material

Supplementary data associated with this article can be found, in the online version, at doi:10.1016/j.ica.2011.05.024.

References

[1] M.K. Tse, C. Dobler, S. Bhor, M. Klawonn, W. Magerlein, H. Hugl, M. Beller, Angew. Chem., Int. Ed. 43 (2004) 5255.
[2] D.V. Deubel, G. Frenking, P.S. Gisdaki, W.A. Herrmann, N. Rosch, J. Sundermeyer, J. Acc. Chem. Res. 37 (2004) 645.
[3] Y. Shi, Acc. Chem. Res. 37 (2004) 488.
[4] M. Hickey, D. Goeddel, Z. Crane, Y. Shi, Proc. Natl. Acad. Sci. USA 101 (2004) 5794.
[5] E.M. McGiarrigle, D.G. Gilheany, Chem. Rev. 105 (2005) 1563.
[6] M.T. Pope, C.K. Jorgensen, et al. (Eds.), Heteropoly and IsopolyOxometalates, Inorganic Chemistry Concepts, vol. 8, Springer Verlag, West Berlin, 1983.
[7] T. Yamase, Catal. Surv. Asia 7 (2003) 226.
[8] J.F. Keggin, Nature 131 (1933) 908.
[9] I.K. Song, M.S. Kaba, M.A. Barteau, Langmuir 18 (2002) 2358.
[10] T. Okuhara, N. Mizuno, M. Misono, Adv. Catal. 41 (1996) 113.
[11] N. Dubey, S.S. Rayalu, N.K. Labhsetwar, S. Devotta, Int. J. Hydrogen Energy 33 (2008) 5958.
[12] T. He, J. Yao, Prog. Mater. Sci. 51 (2006) 810.
[13] J.Y. Niu, X.Z. You, C.Y. Duan, Inorg. Chem. 35 (1996) 4211.
[14] I.V. Kozhevnikov, K.I. Matveev, Appl. Catal. 5 (1983) 135.
[15] M. Misono, Stud. Surf. Sci. Catal. 75 (1993) 69.
[16] C.W. Hu, M. Hashimoto, T. Okuhara, M. Misono, J. Catal. 143 (1993) 437.
[17] C. Venturello, E. Alneri, M. Ricci, J. Org. Chem. 48 (1983) 3831.
[18] C. Venturello, R. D'Aloisio, J.C. Bart, M. Riai, J. Mol. Catal. 32 (1985) 107.
[19] Y. Ishii, K. Yamawaki, T. Yoshida, T. Ura, H. Yamada, M. Ogawe, J. Org. Chem. 52 (1987) 1868.
[20] Y. Ishii, K. Yamawaki, T. Ura, H. Yamada, T. Yoshida, M. Ogawa, J. Org. Chem. 53 (1988) 3587.
[21] R.I. Kureshy, I. Ahmad, N.H. Khan, S.H.R. Abdi, K. Pathak, R.V. Jasra, J. Catal. 238 (2006) 134.
[22] N.K.K. Raj, S.S. Deshpande, R.H. Ingle, T. Raja, P. Manikandan, Stud. Surf. Sci. Catal. 156 (2005) 769.
[23] Z. Karimi, A.R. Mahjoub, Catal. Commun. 12 (2011) 984.
[24] P.J. Collman, L. Zeng, I.J. Brauman, Inorg. Chem. 43 (2004) 2672.
[25] I.V. Kozhevnikov, Catal. Rev. Sci. Eng. 37 (1995) 311.
[26] W. Chu, X. Yang, Y. Shan, X. Ye, Y. Wu, Catal. Lett. 42 (1996) 201.
[27] N.Y. He, C.S. Woo, H.G. Kim, H.I. Lee, Appl. Catal. A 281 (2005) 167.
[28] D. Carriazo, C. Domingo, C. Martín, V. Rives, J. Solid State Chem. 181 (2008) 2046.
[29] A. Bordoloi, F. Lefebvre, S.B. Halligudi, J. Catal. 247 (2007) 166.
[30] D.Y. Zhao, Q.S. Huo, J.L. Feng, B.E. Chmelka, G.D. Stucky, J. Am. Chem. Soc. 120 (1998) 6024.
[31] P. Karandikar, K.C. Dhanya, S. Deshpande, A.J. Chandwadkar, S. Sivasanker, M. Agashe, Catal. Commun. 5 (2004) 69.
[32] F. Ehrburger-Dolle, I. Morfin, E. Geissler, F. Bley, F. Livet, C. Vix-Guterl, S. Saadallah, J. Parmentier, M. Reda, J. Patarin, M. Iliescu, J. Werckmann, Langmuir 19 (2003) 4303.
[33] R. Ryoo, C.H. Ko, M. Kruk, V. Antochshuk, M. Jaroniec, J. Phys. Chem. B 104 (2000) 11465.
[34] X. Wang, K.S.K. Lin, J.C.C. Chan, S. Cheng, J. Phys. Chem. B 109 (2005) 1763.
[35] A.S.M. Chong, X.S. Zhao, J. Phys. Chem. B 107 (2003) 12650.
[36] T. Yokoi, H. Yoshitake, T. Tasumi, Chem. Mater. 15 (2003) 4536.
[37] M.C. Burleigh, M.A. Markowitz, M.S. Spector, B.P. Gaber, Chem. Mater. 13 (2001) 4760.
[38] N.K. Kala Raj, S.S. Deshpande, R.H. Ingle, T. Raja, P. Manikandan, Catal. Lett. 98 (2004) 217.
[39] A. Bordoloi, A. Vinu, S.B. Halligudi, Appl. Catal. A Gen. 333 (2007) 143.
[40] R.D. Birkhoff, J.M. Heller, H.H. Hubbell, L.R. Painter, J. Chem. Phys. 74 (1981) 200.
[41] G. Kraml, G. Gritzner, J. Chem. Soc., Faraday Trans. I 81 (1985) 2875.

[42] R. Massart, R. Contant, J.M. Fruchart, J.P. Ciabrini, M. Fournier, Inorg. Chem. 16 (1977) 2916.
[43] Booth, H.C. (Ed.), Inorganic Syntheses, vol. 1, McGraw Hill, New York, 1939.
[44] Y.H. Guo, C.W. Hu, J. Cluster Sci. 14 (2003) 505.
[45] F. Lefebvre, J. Chem. Soc., Chem. Commun. (1992) 756.
[46] V.M. Mastikhin, S.M. Kulikov, A.V. Nosov, I.V. Kozhevnikov, I.L. Mudrakovsky, M.N. Timofeeva, J. Mol. Catal. 60 (1990) 65.
[47] S. Damyanova, J.L.G. Fierro, I. Sobrados, J. Sanz, Langmuir 15 (1999) 469.
[48] N.A. Stephenson, A.T. Bell, J. Mol. Catal. A 258 (2006) 231.
[49] M.H. Lim, C.F. Blanford, A. Stein, Chem. Mater. 10 (1998) 467.
[50] N.Y. Hea, C.S. Woo, H.G. Kim, H.I. Lee, Appl. Catal. A: General 281 (2005) 167.
[51] B.S. Lane, K. Burgess, Chem. Rev. 103 (2003) 2457.
[52] R. Noyori, M. Aoki, K. Sato, Chem. Commun. (2003) 1977.
[53] D.E. De Vos, B.F. Sels, P.A. Jacobs, Adv. Synth. Catal. 345 (2003) 457.
[54] J.M. Bregeault, Dalton Trans. (2003) 3289.
[55] Z. Karimi, A.R. Mahjoub, F. Davari Aghdam, Inorg. Chim. Acta 362 (2009) 3725.
[56] N. Mizuno, M. Misono, Chem. Rev. 98 (1998) 199.
[57] L. He, H. Li, W. Zhu, J. Guo, X. Jiang, J. Lu, Y. Yan, Ind. Eng. Chem. Res. 47 (2008) 6890.
[58] I.V. Kozhevnikov, Russ. Chem. Rev. 56 (1987) 811.
[59] Z. Karimi, A.R. Mahjoub, Appl. Surf. Sci. 256 (2010) 4473.